

---

# NEURAL PRIOR ESTIMATION: LEARNING CLASS PRIORS FROM LATENT REPRESENTATIONS

---

A PREPRINT

✉ **Masoud Yavari**  
Isfahan, Iran  
masoud.yavari@gmail.com

✉ **Payman Moallem**  
Department of Electrical Engineering  
Faculty of Engineering  
University of Isfahan, Iran  
p\_moallem@eng.ui.ac.ir

February 23, 2026

## ABSTRACT

Class imbalance induces systematic bias in deep neural networks by imposing a skewed effective class prior. This work introduces the Neural Prior Estimator (NPE), a framework that learns feature-conditioned log-prior estimates from latent representations. NPE employs one or more Prior Estimation Modules trained jointly with the backbone via a one-way logistic loss. Under the Neural Collapse regime, NPE is analytically shown to recover the class log-prior up to an additive constant, providing a theoretically grounded adaptive signal without requiring explicit class counts or distribution-specific hyperparameters.

The learned estimate is incorporated into logit adjustment, forming NPE-LA, a principled mechanism for bias-aware prediction. Experiments on long-tailed CIFAR and imbalanced semantic segmentation benchmarks (STARE, ADE20K) demonstrate consistent improvements, particularly for underrepresented classes. NPE thus offers a lightweight and theoretically justified approach to learned prior estimation and imbalance-aware prediction.

**Code:** <https://github.com/masoudya/neural-prior-estimator>

**Keywords** Long-tailed recognition · Class imbalance · Image classification · Semantic segmentation · Logit adjustment · Prior estimation · Deep neural networks · Pixel-level imbalance

## 1 Introduction

Imbalanced datasets, where a small number of classes dominate the training samples while many others are severely underrepresented, are pervasive in real-world recognition tasks and remain a central challenge for modern deep learning systems [1]. When trained on such skewed distributions, standard classifiers tend to overfit head classes, yielding biased decision boundaries and systematically degraded performance on rare categories. Addressing this issue has motivated a broad literature spanning data-level, objective-level, and model-level interventions [2].

Among these directions, distribution-level corrections operating in logit space have emerged as a particularly clean and effective mechanism for mitigating class imbalance. Logit Adjustment (LA) [3] corrects for prior-induced bias by shifting logits according to the logarithm of empirical class frequencies, directly compensating for the mismatch between the training distribution and the desired test-time prior. Integrating this correction into the training objective yields the Logit Adjustment Loss (LAL), which often outperforms post-hoc adjustment by producing a bias-aware classifier end-to-end [3]. These methods are attractive due to their simplicity, theoretical grounding, and compatibility with standard architectures.

However, classical logit adjustment critically relies on access to accurate class priors, typically estimated from dataset-level class counts. This assumption is restrictive in practice. In many realistic scenarios, class distributions evolve over time, are only partially observed, or are distorted by representation learning dynamics. Moreover, empirical class

frequencies do not necessarily reflect the *effective* prior induced by the learned feature space, particularly in deep networks trained under stochastic optimization and finite data regimes.

Several recent works attempt to relax the dependence on explicit priors by learning calibration functions that map logits to a target distribution [4, 5]. While effective, these approaches learn implicit transformations entangled with the classifier outputs and typically require a balanced or curated meta-validation set for supervision. As a result, they do not provide an explicit estimate of the class prior itself, nor can they adapt online in the absence of external calibration data.

In this work, we depart from these restrictive assumptions to explore the autonomous recovery of class priors directly from latent feature representations. We introduce the *Neural Prior Estimator (NPE)*, a lightweight framework designed to derive explicit class log-prior estimates independently of empirical counts or external meta-validation data. The architecture centers on a *Prior Estimation Module (PEM)*, which is optimized via a specialized one-way logistic loss to map the implicit geometric density of intermediate features to a class-frequency signal. Through end-to-end integration with the primary backbone, the NPE characterizes the effective class imbalance in a feature-adaptive manner, thereby obviating the need for explicit histograms, pre-computed priors, or distribution-specific hyperparameters.

The estimated log-prior produced by NPE can be directly integrated into logit adjustment, yielding *NPE-LA*, a fully adaptive imbalance-aware prediction mechanism. In contrast to classical logit adjustment [3], which applies a fixed shift derived from static dataset statistics, NPE-LA dynamically recalibrates logits according to the evolving feature distribution. This makes the approach particularly suitable for non-stationary, online, or streaming settings, where class frequencies and feature geometry change over time.

Importantly, NPE-LA operates purely in logit space and does not modify the sampling strategy, backbone architecture, or representation learning objective. As such, it is broadly complementary to information-enrichment techniques, representation-focused methods, and multi-expert architectures. In contrast, approaches that explicitly rebalance the training distribution through re-sampling alter the effective prior observed by the model and are therefore incompatible with the quantities NPE is designed to estimate. Similarly, methods that directly overwrite classifier priors or logits, such as prior-based LAL or classifier re-training strategies like cRT [6], introduce redundant or conflicting bias corrections when combined with NPE-LA.

The remainder of this paper is organized as follows. Section 2 presents the Neural Prior Estimator framework, detailing the design of the Prior Estimation Module and its optimization via the one-way logistic loss, as well as its integration with logit adjustment. Section 3 describes the experimental setup and benchmarks NPE-LA against state-of-the-art baselines, including classical logit adjustment and classifier re-training, across a range of imbalance ratios. Section 4 reports and analyzes the empirical results, and Section 5 concludes with a discussion of limitations and future directions.

## 2 Methodology

This section details the methodology of the Neural Prior Estimator (NPE) framework. First, the general formulation of the long-tailed learning problem is established. Next, the core estimation mechanism — the Prior Estimation Module (PEM) — and its optimization objective are presented. The imbalance-aware prediction mechanism, NPE-LA, is described in detail thereafter. Theoretical justification is provided in Appendix A.

For clarity of presentation, the exposition is restricted to standard classification settings with class-wise logit vectors. Nonetheless, the framework admits a straightforward extension to outputs of arbitrary shape and dimensionality, permitting applications beyond the vector-valued case.

### 2.1 Problem Setup

Let  $\mathcal{D} = \{(\mathbf{x}_i, y_i)\}_{i=1}^N$  denote the training set, where  $\mathbf{x}_i \in \mathcal{X}$  is an input sample and  $y_i \in \{1, \dots, C\}$  is its corresponding class label.

For each class  $c$ , let  $N_c$  denote the number of samples with label  $c$ , such that  $\sum_{c=1}^C N_c = N$ . The degree of imbalance is quantified by the imbalance ratio

$$\rho = \frac{\max_c N_c}{\min_c N_c}. \quad (1)$$

A large value of  $\rho$  reflects a strongly non-uniform empirical class distribution, which is characteristic of imbalanced datasets.

The baseline approach for this classification task involves a standard classifier consisting of a feature extractor  $f_\theta : \mathcal{X} \rightarrow \mathbb{R}^d$  followed by a linear prediction layer parameterized by  $(\mathbf{W}, \mathbf{b})$ :

$$\mathbf{h} = f_\theta(\mathbf{x}), \quad \mathbf{z} = \mathbf{W}\mathbf{h} + \mathbf{b}, \quad (2)$$

where  $\mathbf{h} \in \mathbb{R}^d$  is the representation and  $\mathbf{z} \in \mathbb{R}^C$  is the logit vector, with  $z_c$  denoting the score associated with class  $c$ . The model is typically trained using the Cross-Entropy (CE) loss:

$$\mathcal{L}_{\text{CE}} = \mathbb{E}_{(\mathbf{x}, y) \sim \mathcal{D}} \left[ -\log \frac{\exp(z_y(\mathbf{x}))}{\sum_{c=1}^C \exp(z_c(\mathbf{x}))} \right]. \quad (3)$$

Bayes’ theorem reveals that minimizing the CE loss corresponds to maximizing the log-likelihood of the posterior  $p_\theta(y|\mathbf{x})$ , which decomposes as

$$\log p_\theta(y|\mathbf{x}) = \log p_\theta(\mathbf{x}|y) + \log p(y) + \text{const}. \quad (4)$$

Since neural classifiers implement decision rules in logit space, the empirical class prior  $p(y)$  enters the decision function through its logarithm. Under severe imbalance, differences in  $\log p(y)$  induce substantial implicit additive biases on the logits [3], causing the model to systematically overestimate head classes and underestimate tail classes.

Standard logit adjustment methods mitigate this bias by adding a static global offset computed from the empirical class prior. The usefulness of this fixed intervention, however, is constrained by the limited availability and reliability of the underlying prior. These constraints arise when the effective class distribution drifts over time, when sampling or augmentation procedures modify class frequencies in a data-dependent manner, or when explicit counting of class occurrences is impractical due to the scale or structure of the dataset. To overcome these difficulties, the Neural Prior Estimator is introduced. It Provides a learned, feature-dependent estimate of the implicit class prior derived from intermediate representations, enabling adaptive treatment of non-stationary or feature-conditioned distributions.

## 2.2 Neural Prior Estimator (NPE)

The NPE framework is realized through the integration of one or more Prior Estimation Modules (PEMs), which are trained jointly with the classifier backbone.

**Prior Estimation Modules (PEMs).** Each PEM implements a differentiable mapping from the backbone feature vector to a class-wise output:

$$\mathbf{u}_k(\mathbf{x}) = g_k(\mathbf{h}(\mathbf{x})), \quad k = 1, \dots, N_{\text{PEM}}, \quad (5)$$

where  $\mathbf{u}_k(\mathbf{x}) \in \mathbb{R}^C$  matches the dimensionality of the main classifier logits  $\mathbf{z}(\mathbf{x})$ . Each PEM produces a vector of class-wise values reflecting the observed structure in the training data. In practice, a single linear mapping from features to  $C$  coordinates is sufficient, though deeper or more complex architectures can also be used without changing the fundamental properties of the NPE framework.

**Training objective.** The loss for each PEM is defined as a one-way logistic term evaluated only on the true-class coordinate. The total NPE objective is the sum of the expected losses across all  $N_{\text{PEM}}$  modules:

$$\mathcal{L}_{\text{NPE}} = \sum_{k=1}^{N_{\text{PEM}}} \mathbb{E}_{(\mathbf{x}, y) \sim \mathcal{D}} [-\log \sigma((-1)^t u_k(\mathbf{x})_y)], \quad (6)$$

where  $\sigma(u) = (1 + e^{-u})^{-1}$  and  $t \in \{0, 1\}$  determines the sign convention of the update.

For the prediction task, the overall objective combines the CE loss of the main classifier with the NPE loss:

$$\mathcal{L} = \mathcal{L}_{\text{CE}} + \mathcal{L}_{\text{NPE}}. \quad (7)$$

This formulation allows the classifier and all PEMs to be optimized jointly, with the feature extractor receiving gradient signals from both objectives throughout training.

**Emergent frequency-dependent structure.** The one-way logistic loss affects only the true-class coordinate, enforcing a fixed update direction—positive when  $t = 0$  and negative when  $t = 1$ . Gradient contributions along this coordinate accumulate over training in proportion to the frequency of the corresponding class, yielding PEM outputs whose scale naturally encodes the empirical class distribution and giving rise to a characteristic frequency-dependent structure.

**NPE estimate** To consolidate the outputs of the PEMs into a single classwise estimate, the *NPE estimate* is defined as:

$$\boldsymbol{\eta}(\mathbf{x}) = \frac{(-1)^t}{N_{\text{PEM}}} \sum_{k=1}^{N_{\text{PEM}}} \mathbf{u}_k(\mathbf{x}). \quad (8)$$

Here,  $(-1)^t$  enforces a consistent sign convention independent of the training choice of  $t$ , and the normalization by  $N_{\text{PEM}}$  ensures that the scale of  $\boldsymbol{\eta}(\mathbf{x})$  is invariant to the number of PEMs.

This mapping constitutes the operational definition of the Neural Prior Estimator. A theoretical analysis in Appendix A demonstrates that, under general assumptions, the NPE estimate converges toward a monotone transformation of the empirical class counts, thereby capturing the underlying class distribution up to a small, controlled deviation.

**Equivalence of estimating  $\log N_c$  and  $\log p_c$ .** As shown in Appendix A, PEM optimization converges to values proportional to  $\log N_c$ . The true class prior satisfies

$$p_c = \frac{N_c}{\sum_j N_j}, \quad (9)$$

which can be rewritten as

$$\log p_c = \log N_c - \log \left( \sum_j N_j \right), \quad (10)$$

where the second term is a class-independent constant. Therefore, estimating  $\log N_c$  is equivalent to estimating  $\log p_c$  up to an additive shift, establishing the NPE framework as a method for *log-prior estimation*.

**Number of PEMs.** A single PEM is fully sufficient for constructing the NPE estimate. The framework allows  $N_{\text{PEM}} > 1$  primarily to support downstream applications in which multiple PEMs can influence the backbone through their combined gradients. This flexibility does not alter the definition of NPE itself.

**Number of PEMs.** A single PEM is sufficient for constructing the NPE estimate, and increasing the number of PEMs does not alter its definition. Allowing  $N_{\text{PEM}} > 1$  modifies only the gradient signals received by the shared backbone. Because saturation under the one-way logistic loss depends on class frequency, each PEM contributes class-dependent gradients whose persistence varies across classes. Multiple independently initialized PEMs therefore amplify and distribute these class-wise signals through their combined updates, affecting the backbone’s optimization trajectory without changing the underlying NPE formulation.

**Choice of sign convention.** The parameter  $t$  determines the direction of the update applied to the true-class coordinate. The NPE estimate is automatically re-signed, so its final value is invariant to this choice. Empirically, the subtractive configuration ( $t = 1$ ) performs favorably and is adopted in all subsequent experiments.

### 2.3 NPE for Imbalance-Aware Prediction

Since  $\log N_c$  and  $\log p_c$  differ only by a class-independent constant, the NPE estimate  $\boldsymbol{\eta}(\mathbf{x})$  can be used directly as an estimate of the log prior (up to shift). Accordingly, NPE-LA applies  $\boldsymbol{\eta}(\mathbf{x})$  as a feature-conditioned prior correction:

$$\tilde{\mathbf{z}}(\mathbf{x}) = \mathbf{z}(\mathbf{x}) - \boldsymbol{\eta}(\mathbf{x}). \quad (11)$$

The procedure is structurally related to classical logit adjustment [3], but differs in two key aspects. First, the effective prior is *learned jointly* during training rather than fixed in advance. Second, the correction is *feature-dependent*: the adjustment responds to the local behavior of the representation  $\mathbf{h}(\mathbf{x})$ .

**Inference-Time Efficiency.** When both the main classifier and all PEMs are linear, the adjustment can be expressed as a single equivalent linear classifier obtained by combining their weights and biases. Thus, NPE-LA introduces no additional inference-time cost and requires no architectural modifications at deployment.

## 3 Experiments

This section describes the experimental setup used to evaluate NPE-LA across different tasks. Both image-level classification on CIFAR datasets and pixel-level semantic segmentation on STARE and ADE20K are considered. The experiments are designed to assess performance under imbalanced class distributions.

All PEMs are initialized with a normal distribution having a small standard deviation of 0.001, ensuring that the initial NPE estimate is close to zero. This choice prevents the one-way logistic loss from operating in a saturated regime at the start of training, preserving informative gradients and avoiding early optimization collapse.

Table 1: Training hyperparameters for classification experiments. LR decay factor = 0.1 at each milestone.

Setting	LR	Weight Decay	Batch Size	Epochs	LR decay milestones
HP-1	0.1	$2 \times 10^{-4}$	124	200	160, 180
HP-2	0.05	$10^{-3}$	64	120	100, 110

Table 2: Per-model training schedule and optimizer settings. LR decay factor = 0.1 at each milestone.

Dataset	Backbone + Head	Optimizer	LR	WD	Iterations	LR decay milestones
STARE	UNet-FCN	SGD	1e-2	5e-4	600	200, 400
ADE20K	DeepLab-V3	SGD	1e-2	5e-4	2 500	1 250
ADE20K	Swin-T + UPerNet	AdamW	6e-5	1e-2	2 500	1 250

### 3.1 Classification Experiments

NPE-LA is evaluated on long-tailed CIFAR-10 and CIFAR-100 [7] using a ResNet-32 backbone [8] trained from scratch with SGD (momentum 0.9) and standard data augmentation. Classes are grouped by sample count: Head classes contain more than 100 samples, Medium classes contain between 20 and 100 samples, and Tail classes contain fewer than 20 samples.

Robustness to training conditions is assessed using two hyperparameter configurations summarized in Table 1. HP-1 follows the settings introduced in [9], which are widely used in imbalance-aware prediction studies, while HP-2 is a custom configuration designed to examine sensitivity to different optimization dynamics. NPE-LA is compared against CE, cRT, and LAL under identical conditions. All reported results are mean  $\pm$  std across three independent runs, and final-epoch accuracy is used as the evaluation metric.

### 3.2 Semantic Segmentation Experiments

NPE-LA is evaluated on semantic segmentation using two imbalanced datasets: STARE [10] and ADE20K [11]. STARE contains 20 retinal images with two classes, where vessel pixels comprise only about 14% of the image, creating a pronounced pixel-level imbalance. ADE20K includes 20,000 images and 150 categories with substantial frequency skew, with some classes appearing infrequently.

Pretrained backbones and decoder heads from MMSegmentation [12] are used and kept frozen during PEM training. Freezing the feature extractor isolates the effect of the PEM and ensures that performance changes stem solely from logit recalibration rather than altered representations. For STARE, a UNet [13] with an FCN head [14] is used, while ADE20K experiments employ either DeepLabv3 [15] or Swin-T [16] paired with a UPerNet decoder [17]. Optimizer hyperparameters, including learning rate, momentum, and weight decay, follow MMSegmentation defaults, and the total training iterations and learning-rate decay schedule follow the custom configuration in Table 2.

To examine how architectural capacity influences logit recalibration, two PEM variants are considered. The first is a minimal, single-layer FCN which yields a purely linear feature-to-estimate mapping. The second variant replicates the structure of the main decoder head, thereby introducing non-linear transformations. These two designs allow for a rigorous analysis of NPE across both linear and non-linear estimator modules and under different levels of representational complexity.

**Omission of Batch Normalization.** Batch Normalization (BN) is intentionally omitted at the NPE estimate because the PEM output ( $\mathbf{u}_k(\mathbf{x})$ ) are designed to encode scale information reflecting class-frequency-dependent adjustments. Applying BN would remove this critical scale information, destabilizing optimization and undermining the NPE’s role as a prior estimator.

**Scaling for Dense Prediction.** In dense prediction tasks (e.g., semantic segmentation), the main segmentation head typically applies BN, which normalizes each output channel independently across all pixels in the batch. For imbalanced classes, this normalization artificially amplifies rare-class channels while compressing dominant-class channels. For instance, a rare-class channel (e.g., small lesions) is forced to unit variance similar to a dominant background channel, effectively scaling up its prediction strength relative to its frequency.

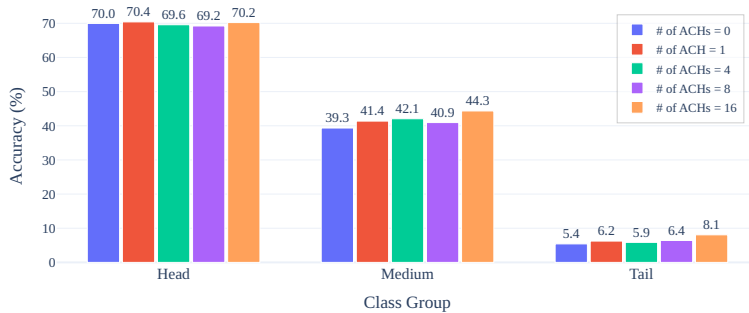


Figure 1: Class-wise accuracy on CIFAR-100 ( $\rho = 100$ ) under HP-2, illustrating the impact of different numbers of PEMs ( $N_{\text{PEM}}$ ) across Head, Medium, and Tail classes. NPE is utilized during training only; no logit adjustment is performed at inference time.

Directly combining these BN-normalized main logits with the unnormalized NPE estimate would therefore excessively inflate rare-class predictions, potentially causing boundary bleeding and increasing false positives. To prevent this, a scalar scaling factor  $\alpha$  is applied to the aggregated PEM correction:

$$\eta_{\text{scaled}}(\mathbf{x}) = \alpha \eta(\mathbf{x}),$$

where  $\alpha < 1$  dampens the prior correction to match the scale of the main-head logits. This preserves the relative class-frequency adjustments while maintaining stable dense predictions and optimizing intersection-based metrics such as mIoU.

## 4 Results and Discussion

This section presents an empirical evaluation of the Neural Prior Estimator framework. The analysis begins by examining the regularization effect induced by PEMs on the backbone, then evaluates the full NPE+LA mechanism on long-tailed classification under varying optimization regimes, and finally considers its application to semantic segmentation.

### 4.1 Classification Results

Before evaluating the full NPE-LA framework, we isolate the implicit impact of the NPE training objective on the shared feature backbone. In this ablation, the PEMs are active only during training; at inference time, the standard classifier is used without any logit adjustment.

Models were trained deterministically with varying numbers of PEMs ( $N_{\text{PEM}} \in \{0, 1, 4, 8, 16\}$ ). Figure 1 illustrates the resulting mean accuracy across Head, Medium, and Tail subgroups on CIFAR-100 ( $\rho = 100$ ).

Increasing the number of PEMs during training demonstrates a clear positive effect on Medium and Tail class performance. Introducing even a single PEM yields measurable gains for both groups, while adding additional heads further amplifies these improvements. In contrast, Head-class accuracy remains largely stable across all configurations. This behavior empirically supports the mechanism described in Section 2.2: the one-way logistic loss produces class-dependent gradients that persist for under-represented classes, subtly perturbing the backbone features to support improved tail-class generalization.

Table 3 reports the mean accuracy on CIFAR-100 and CIFAR-10 for the same experimental setting. Introducing PEMs generally improves overall accuracy, with diminishing returns as the number of heads grows. In practice, the optimal number of PEMs depends on dataset complexity, imbalance severity, and model capacity; simpler datasets or low imbalance ratios tend to benefit from fewer heads, whereas more complex datasets or higher imbalance ratios can take advantage of a larger PEM ensemble.

Following the analysis of PEM-only training, the next experiments evaluate the full NPE-LA mechanism, where the learned prior offsets are applied during inference. Classification performance on CIFAR-100 and CIFAR-10 under hyperparameter settings HP-1 and HP-2 is reported in Table 4 and Table 5, respectively.

A consistent pattern emerges across both hyperparameter settings. Under HP-1, NPE-LA matches or surpasses the strongest baseline, LA, in nearly all scenarios. The configuration with 16 PEMs delivers the most reliable improvements,

Table 3: Top-1 accuracy (%) on CIFAR-100 and CIFAR-10 for different imbalance ratios  $\rho$  and PEMs under hyperparameter setting HP-2. NPE is utilized during training only; no logit adjustment is performed at inference time.

# of PEMs	CIFAR-100			CIFAR-10		
	200	100	50	200	100	50
0	37.62	40.53	45.98	64.40	<b>75.01</b>	77.00
1	37.28	41.00	45.96	65.24	73.05	78.29
4	37.09	<b>42.35</b>	45.45	<b>66.31</b>	73.95	77.99
8	38.39	41.65	46.29	66.13	73.72	<b>78.98</b>
16	<b>38.42</b>	41.78	<b>46.36</b>	66.22	74.20	78.33

Table 4: Top-1 accuracy (%) on CIFAR-100 and CIFAR-10 for different imbalance ratios  $\rho$  and methods under hyperparameter setting HP-1. Bold indicates the highest value; underlined indicates the second highest

Method	CIFAR-100			CIFAR-10		
	200	100	50	200	100	50
CE	34.83 $\pm$ 0.26	39.14 $\pm$ 0.41	43.87 $\pm$ 0.25	63.54 $\pm$ 0.28	71.24 $\pm$ 0.29	76.77 $\pm$ 0.37
cRT	37.04 $\pm$ 0.24	41.04 $\pm$ 0.14	45.83 $\pm$ 0.32	67.19 $\pm$ 0.31	73.80 $\pm$ 0.42	79.07 $\pm$ 0.51
LA	38.59 $\pm$ 0.18	<u>42.63</u> $\pm$ 0.46	<b>47.07</b> $\pm$ 0.49	72.10 $\pm$ 0.27	77.37 $\pm$ 0.32	81.25 $\pm$ 0.38
NPE-LA (1 PEM)	<u>38.85</u> $\pm$ 0.30	42.53 $\pm$ 0.40	<u>46.86</u> $\pm$ 0.78	<u>72.42</u> $\pm$ 0.21	<u>77.89</u> $\pm$ 0.38	<u>82.22</u> $\pm$ 0.46
NPE-LA (16 PEMs)	<b>39.36</b> $\pm$ 0.12	<b>42.73</b> $\pm$ 0.28	46.44 $\pm$ 0.24	<b>73.18</b> $\pm$ 0.41	<b>78.17</b> $\pm$ 0.73	<b>82.31</b> $\pm$ 0.22

Table 5: Top-1 accuracy (%) on CIFAR-100 and CIFAR-10 for different imbalance ratios  $\rho$  and methods under hyperparameter setting HP-2. Bold indicates the highest value; underlined indicates the second highest

Method	CIFAR-100			CIFAR-10		
	200	100	50	200	100	50
CE	37.04 $\pm$ 0.23	41.00 $\pm$ 0.12	45.46 $\pm$ 0.11	65.59 $\pm$ 0.20	73.18 $\pm$ 0.77	77.76 $\pm$ 0.44
cRT	41.58 $\pm$ 0.24	45.43 $\pm$ 0.11	50.50 $\pm$ 0.12	72.34 $\pm$ 0.71	77.85 $\pm$ 0.25	81.01 $\pm$ 0.50
LA	<u>43.35</u> $\pm$ 0.33	<u>46.85</u> $\pm$ 0.53	<u>51.30</u> $\pm$ 0.22	<b>74.91</b> $\pm$ 0.51	<b>80.13</b> $\pm$ 0.13	<u>82.95</u> $\pm$ 0.36
NPE-LA (1 PEM)	42.99 $\pm$ 0.30	46.72 $\pm$ 0.23	51.25 $\pm$ 0.36	74.37 $\pm$ 0.25	79.35 $\pm$ 0.37	82.32 $\pm$ 0.19
NPE-LA (16 PEMs)	<b>43.96</b> $\pm$ 0.40	<b>47.47</b> $\pm$ 0.36	<b>51.82</b> $\pm$ 0.17	<u>74.83</u> $\pm$ 0.55	<u>80.12</u> $\pm$ 0.31	<b>83.16</b> $\pm$ 0.08

especially under severe imbalance ( $\rho = 200$ ), where gains over CE and cRT are substantial. While LA retains a slight edge in a few mid-range cases, NPE-LA with a single PEM remains competitive and typically achieves the second-best results.

Under HP-2, where the backbone trains more effectively and all methods achieve higher absolute accuracy, the advantage of NPE-LA becomes clearer. With 16 PEMs, the method outperforms all baselines on CIFAR-100 for every imbalance ratio, including milder settings such as  $\rho=50$ . On CIFAR-10 the gap naturally shrinks due to the dataset’s simplicity, yet NPE-LA still yields the best or second-best performance throughout, exceeding LA at  $\rho=50$  and matching it closely elsewhere.

Comparing the two tables shows that NPE-LA delivers markedly larger gains under HP-1 than HP-2, with the gap widening most at high imbalance ratios (notably  $\rho=200$ ). The large batch size in HP-1 intensifies gradient dominance from head classes, suppressing updates for tail classes; in this setting, PEM-induced backbone perturbations yield much stronger benefits. Under HP-2, the smaller batch size mitigates this gradient imbalance, improving the optimization landscape for all methods and narrowing NPE-LA’s relative advantage. This contrast indicates that NPE-LA is most impactful when tail-class gradients are most heavily suppressed.

Figure 2 shows class-wise accuracy on CIFAR-100 for the high-imbalance setting ( $\rho = 100$ ) under HP-2. CE prioritizes head classes, leaving tail categories largely unrecognized. cRT shifts performance toward minority classes, improving medium and tail accuracy at the expense of head performance. LA pushes this redistribution further, providing the strongest tail gains among the baselines while imposing the largest reduction on head classes. NPE-LA moves in the same direction but achieves a more favorable balance. NPE-LA with even a single PEM outperforms cRT on medium and tail classes, albeit with lower performance on the head classes. Employing sixteen PEMs brings tail-class accuracy close to that of LA while achieving a more balanced overall performance.

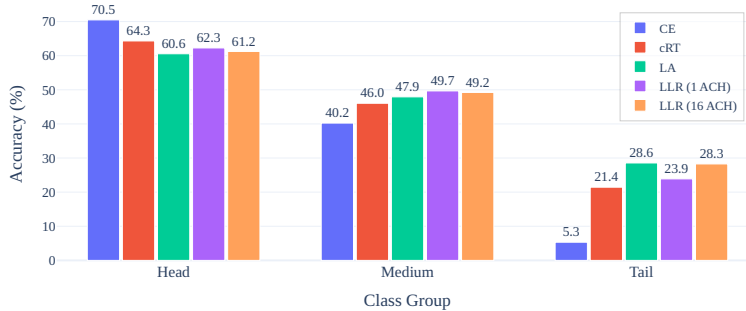


Figure 2: Class-wise accuracy on CIFAR-100 ( $\rho = 100$ ) under HP-2, comparing different methods across head, medium, and tail classes.

Table 6: STARE segmentation with UNet–FCN: Dice and pixel accuracy for background (BG), foreground (FG), and mean, comparing the baseline and NPE-LA across scale factors  $\alpha$ .

Backbone	Decode Head	PEM Type	Scale Factor	Dice (%)			Accuracy (%)		
				BG	FG	Mean	BG	FG	Mean
UNet	FCN	-	-	<b>98.55</b>	81.20	89.78	<b>99.13</b>	75.21	87.17
		FCN	1	97.34	75.02	86.27	95.22	<b>94.93</b>	<b>95.08</b>
			0.2	98.52	<b>82.39</b>	<b>90.46</b>	98.44	83.21	90.83

## 4.2 Segmentation Results

In contrast to the classification experiments, the segmentation experiments are conducted with a frozen backbone. This constraint implies that the NPE does not influence the shared backbone features, leading to the evaluation of NPE-LA exclusively in a single PEM configuration.

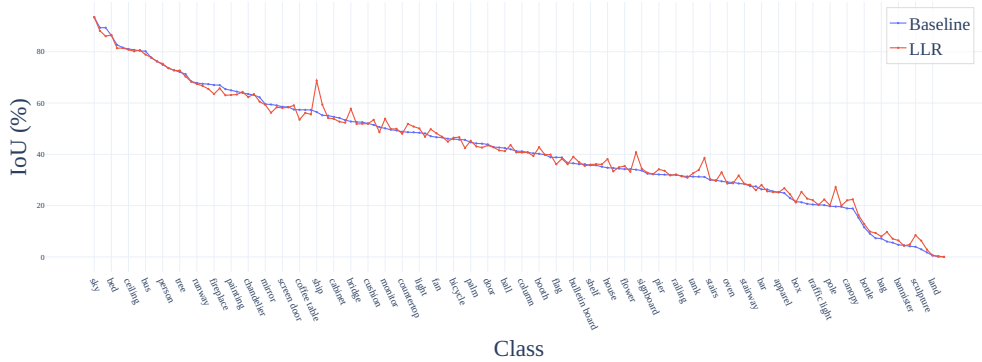
The segmentation performance on the STARE dataset with a UNet backbone under different scale factors is summarized in Table 6. Introducing NPE-LA with a large scale factor shifts the decision boundary toward the underrepresented foreground class, leading to a notable increase in foreground accuracy, albeit with a decrease in mean Dice due to its sensitivity to overprediction on small structures. Increasing the scale factor results in a more balanced recalibration, maintaining background stability while improving both mDice and mAcc beyond the baseline. These results demonstrate that NPE-LA effectively captures pixel-wise prior information. Results on the complex ADE20K dataset reproduce the trends observed on STARE, demonstrating the consistent behavior of NPE-LA across different backbone and decoder architectures (Table 7). For DeepLab-V3, scaled NPE-LA restores mIoU to baseline levels while improving mAcc. The ASPHead configuration yields a larger mAcc gain than the FCN variant; nevertheless, the FCN PEM still provides measurable improvement despite being a simple, single-layer module. For the Swin-T backbone with the complex UPerNet PEM, an unscaled recalibration drastically reduces both mIoU and mAcc. This pronounced degradation, particularly in mAcc, arises because UPerNet’s pyramid design causes the NPE to capture both local and global context for pixel prior estimation. Consequently, unscaled logit adjustment can produce not only localized boundary errors but also global overcorrection across the pixel map. Applying an appropriate scaling factor restores stability and enables modest gains. Although the improvement over the Swin-T baseline is limited, this experiment primarily demonstrates that NPE-LA can be successfully integrated across contemporary architectures and optimization schemes (AdamW), rather than evaluating absolute performance gains.

Figure 3 show class-wise accuracy and IoU for baseline DeepLab-V3 and the NPE-LA variant with an FCN PEM and scale factor of 0.1. IoU decreases slightly for classes that already perform well but increases for weaker classes. Class-wise accuracy generally improves, reflecting NPE-LA’s effect of redistributing confidence without destabilizing overall predictions.

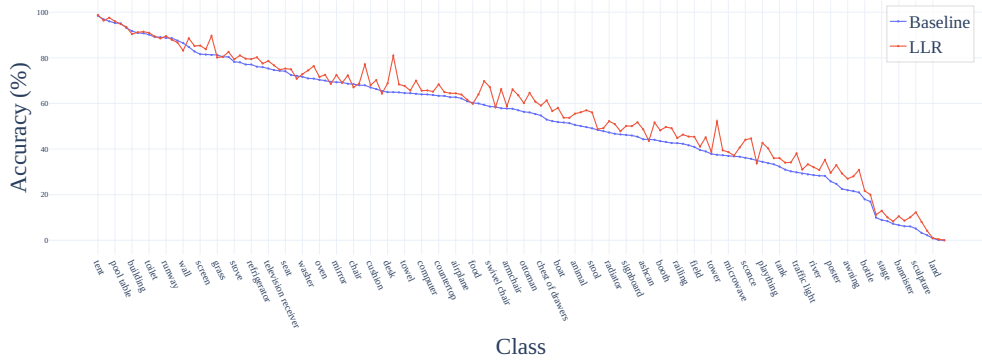
Overall, the STARE and ADE20K experiments suggest that NPE-LA can adjust predictions for underrepresented classes while maintaining stable performance for the main decoder, even with simple PEM configurations and frozen backbones.

Table 7: ADE20K segmentation with DeepLabv3 and Swin-T: mIoU and pixel accuracy for baseline and NPE-LA with different PEM types and scale factors  $\alpha$ .

Backbone	Decode Head	PEM Type	Scale Factor	mIoU (%)	mAcc (%)
		-	-	42.42	53.60
DeepLab-V3	ASPPHead	ASPPHead	1	24.55	65.59
			0.1	42.82	57.99
		FCN	1	29.28	67.05
			0.1	42.92	56.92
<hr/>					
		-	-	44.41	55.96
Swin-T	UpperNet	UpperNet	1	12.29	32.51
			0.1	42.15	62.73
		FCN	1	33.87	66.51
			0.1	44.73	58.00



(a) Class-wise IoU



(b) Class-wise accuracy

Figure 3: Class-wise IoU and accuracy on ADE20K for baseline DeepLab-V3 and NPE-LA (single FCN PEM,  $\alpha = 0.1$ ). Classes are ordered by ascending baseline performance for clarity.

## 5 Conclusion

This work introduced the Neural Prior Estimator (NPE) framework, a principled approach for estimating implicit class priors directly from feature representations. NPE employs lightweight Prior Estimation Modules (PEMs) trained with a one-way logistic loss, a mechanism that enables class-dependent logit biases to emerge naturally and adaptively.

Theoretical analysis demonstrated that, under idealized conditions, NPE approximate the log-prior, while empirical evaluations confirmed their fidelity across realistic datasets and revealed systematic interactions with feature geometry.

Building on these learned priors, we proposed NPE-LA, which integrates NPE with standard logit adjustment. Aggregated PEM outputs provide feature-adaptive logit offsets added to classifier logits at inference, thereby aligning decision boundaries in a representation-aware manner. This design is minimally intrusive, preserves the backbone architecture, and introduces negligible computational overhead, making it readily compatible with existing augmentation and representation-enhancement methods.

Extensive experiments on long-tailed CIFAR benchmarks showed that NPE-LA consistently improves performance for tail and minority classes while maintaining competitive overall accuracy relative to conventional logit adjustment and classifier re-training. Furthermore, the framework successfully generalizes to dense prediction tasks: when applied to semantic segmentation benchmarks (STARE and ADE20K), PEM-based offsets provide modest yet measurable pixel-level recalibration, yielding notable gains for rare categories.

Beyond imbalance-aware classification, NPE provides a general mechanism for extracting effective class-frequency signals from latent representations. Promising directions include label-shift adaptation, adaptive reweighting schemes driven by feature-space density, and integration with multi-expert or ensemble systems where prior estimates may guide expert selection. Exploring these extensions in structured prediction, streaming settings, and other distribution-shift scenarios remains future work.

In summary, NPE provides a theoretically grounded, flexible, and practically efficient mechanism for learning and leveraging class priors, and when combined with logit adjustment, it offers a robust and state-of-the-art solution for mitigating class imbalance in both instance-level and dense prediction tasks.

## References

- [1] Chongsheng Zhang, George Alpanidis, Gaojuan Fan, Binqun Deng, Yanbo Zhang, Ji Liu, Aouaidjia Kamel, Paolo Soda, and João Gama. A systematic review on long-tailed learning. *IEEE Transactions on Neural Networks and Learning Systems*, 2025.
- [2] Yifan Zhang, Bingyi Kang, Bryan Hooi, Shuicheng Yan, and Jiashi Feng. Deep long-tailed learning: A survey. *IEEE transactions on pattern analysis and machine intelligence*, 45(9):10795–10816, 2023.
- [3] Aditya Krishna Menon, Sadeep Jayasumana, Ankit Singh Rawat, Himanshu Jain, Andreas Veit, and Sanjiv Kumar. Long-tail learning via logit adjustment. *arXiv preprint arXiv:2007.07314*, 2020.
- [4] Junjiao Tian, Yen-Cheng Liu, Nathaniel Glaser, Yen-Chang Hsu, and Zsolt Kira. Posterior re-calibration for imbalanced datasets. *Advances in neural information processing systems*, 33:8101–8113, 2020.
- [5] Songyang Zhang, Zeming Li, Shipeng Yan, Xuming He, and Jian Sun. Distribution alignment: A unified framework for long-tail visual recognition. In *Proceedings of the IEEE/CVF conference on computer vision and pattern recognition*, pages 2361–2370, 2021.
- [6] Bingyi Kang, Saining Xie, Marcus Rohrbach, Zhicheng Yan, Albert Gordo, Jiashi Feng, and Yannis Kalantidis. Decoupling representation and classifier for long-tailed recognition. *arXiv preprint arXiv:1910.09217*, 2019.
- [7] Alex Krizhevsky, Geoffrey Hinton, et al. Learning multiple layers of features from tiny images. 2009.
- [8] Kaiming He, Xiangyu Zhang, Shaoqing Ren, and Jian Sun. Deep residual learning for image recognition. In *Proceedings of the IEEE conference on computer vision and pattern recognition*, pages 770–778, 2016.
- [9] Kaidi Cao, Colin Wei, Adrien Gaidon, Nikos Archiga, and Tengyu Ma. Learning imbalanced datasets with label-distribution-aware margin loss. *Advances in neural information processing systems*, 32, 2019.
- [10] AD Hoover, Valentina Kouznetsova, and Michael Goldbaum. Locating blood vessels in retinal images by piecewise threshold probing of a matched filter response. *IEEE Transactions on Medical imaging*, 19(3):203–210, 2000.
- [11] Bolei Zhou, Hang Zhao, Xavier Puig, Sanja Fidler, Adela Barriuso, and Antonio Torralba. Scene parsing through ade20k dataset. In *Proceedings of the IEEE conference on computer vision and pattern recognition*, pages 633–641, 2017.
- [12] MMSegmentation Contributors. MMSegmentation: Openmmlab semantic segmentation toolbox and benchmark. <https://github.com/open-mmlab/mms Segmentation>, 2020.
- [13] Olaf Ronneberger, Philipp Fischer, and Thomas Brox. U-net: Convolutional networks for biomedical image segmentation. In *International Conference on Medical image computing and computer-assisted intervention*, pages 234–241. Springer, 2015.

- 
- [14] Jonathan Long, Evan Shelhamer, and Trevor Darrell. Fully convolutional networks for semantic segmentation. In *Proceedings of the IEEE conference on computer vision and pattern recognition*, pages 3431–3440, 2015.
  - [15] Liang-Chieh Chen, George Papandreou, Florian Schroff, and Hartwig Adam. Rethinking atrous convolution for semantic image segmentation. *arXiv preprint arXiv:1706.05587*, 2017.
  - [16] Ze Liu, Yutong Lin, Yue Cao, Han Hu, Yixuan Wei, Zheng Zhang, Stephen Lin, and Baining Guo. Swin transformer: Hierarchical vision transformer using shifted windows. *arXiv preprint arXiv:2103.14030*, 2021.
  - [17] Tete Xiao, Yingcheng Liu, Bolei Zhou, Yuning Jiang, and Jian Sun. Unified perceptual parsing for scene understanding. In *Proceedings of the European conference on computer vision (ECCV)*, pages 418–434, 2018.
  - [18] Vardan Papyan, XY Han, and David L Donoho. Prevalence of neural collapse during the terminal phase of deep learning training. *Proceedings of the National Academy of Sciences*, 117(40):24652–24663, 2020.

## A Theoretical Analysis of Prior Estimation

This section analyzes, under a simplified but analytically tractable model, the behavior of a *single* Prior Estimation Module (PEM) trained with the one-way logistic loss. The goal is to characterize the dominant class-dependent structure learned by the PEM logits and establish that they approximate the *log-prior*. This analysis is independent of architectural details and does not assume linearity of the PEM. Instead, it focuses solely on the scalar logits emitted for each class.

To obtain a closed-form solution, the derivation relies on the *Neural Collapse* (NC) regime [18], where features of all samples in class  $c$  are mapped to the same PEM logit  $\eta_c$ . This reduction allows the PEM objective to be expressed as a convex one-dimensional optimization per class.

### A.1 Model Setup

Let  $\mathcal{D} = \{(\mathbf{x}_i, y_i)\}_{i=1}^N$  denote the training set, with  $N_c$  samples from class  $c$ , giving empirical prior  $p(c) = N_c/N$ . Under NC, the NPE estimate for class  $c$  is a scalar logit  $\eta_c$ . The one-way logistic loss of logits for an NPE with a single PEM takes the form:

$$J(\boldsymbol{\eta}) = \sum_{c=1}^C \left[ -N_c \log \sigma(\eta_c) + \frac{\lambda}{2} \eta_c^2 \right], \quad (12)$$

where the first term is the logistic loss (under NC), and the second term is the quadratic PEM regularizer. Since PEMs function independently across classes, it suffices to analyze the per-class objective:

$$J_c(\eta) = -N_c \log \sigma(\eta) + \frac{\lambda}{2} \eta^2. \quad (13)$$

This formulation isolates the *prior-dependent* term  $N_c$  from other training dynamics. While real networks exhibit complex feature interactions, the NC model accurately describes late-phase behavior, allowing analytical quantification of the NPE estimate toward empirical class frequency.

### A.2 Closed-Form Minimizer and Asymptotics

**Proposition 1 (Closed-Form Optimal Logit and Asymptotics)** *The unique minimizer of  $J_c$  is*

$$\eta_c^* = W\left(\frac{N_c}{\lambda}\right), \quad (14)$$

where  $W(\cdot)$  denotes the principal branch of the Lambert  $W$  function.

In the saturation regime  $N_c/\lambda \rightarrow \infty$ , the asymptotic expansion is:

$$\eta_c^* = \log\left(\frac{N_c}{\lambda}\right) - \log \log\left(\frac{N_c}{\lambda}\right) + o(1). \quad (15)$$

**proof 1** *Differentiating  $J_c$  and setting the gradient to zero:*

$$\frac{\partial J_c}{\partial \eta} = -N_c \sigma(-\eta) + \lambda \eta = 0.$$

Let  $\eta_c^* = x_c > 0$ . Then

$$N_c e^{-x_c} = \lambda x_c \iff x_c e^{x_c} = \frac{N_c}{\lambda}.$$

By definition,  $x_c = W(N_c/\lambda)$ , so  $\eta_c^* = W(N_c/\lambda)$ .

Convexity follows from  $J_c''(\eta) = N_c \sigma(\eta)(1 - \sigma(\eta)) + \lambda > 0$  for  $\lambda > 0$ .

The asymptotic expansion uses the standard property:  $W(z) = \log z - \log \log z + o(1)$  as  $z \rightarrow \infty$ .

### A.3 Decomposition and Interpretation of the Class-Dependent Residual

Substituting  $N_c = Np(c)$  gives:

$$\eta_c^* = \log p(c) + C_0 + \varepsilon_c, \quad (16)$$

where

$$C_0 = -\log \lambda + \log N, \quad \varepsilon_c = -\log \log\left(\frac{N_c}{\lambda}\right) + o(1).$$

Interpretation:

- **Dominant term**  $\log p(c)$ : The class-dependent component approximating the log-prior.
- **Global constant**  $C_0$ : A class-agnostic shift. When logits are subsequently normalized (e.g., via softmax), this constant cancels and does not affect the predicted class probabilities.
- **Slow-varying remainder**  $\varepsilon_c$ : Doubly logarithmic in  $N_c$ , negligible unless extreme imbalance.

Thus, the PEM output is a monotone transformation of the empirical class frequency, recovering the log-prior up to small corrections.

#### A.4 Implications

Under the Neural Collapse (NC) regime with quadratic regularization, the NPE estimate obtained from a single module closely tracks the empirical class log-prior. This establishes a first-principles justification of NPE as a feature-dependent log-prior estimator, up to an additive constant and a small correction. Notably, this behavior arises directly from the one-way logistic optimization dynamics and does not rely on architectural constraints or linearity assumptions.